

Anomalous Normal State Transport in Underdoped Cuprates: A Preformed-Pair Alternative to the Vortex Scenario

Shina Tan and K. Levin

James Franck Institute and Department of Physics, University of Chicago, Chicago, Illinois 60637

We address those puzzling experiments in underdoped high T_c superconductors which have been associated with normal state “vortices” and show these data can be understood as deriving from preformed pairs with onset temperature $T^* > T_c$. For uncorrelated bosons in small magnetic fields, and arbitrary T^*/T_c , we present the exact contribution to *all* transport coefficients. In the overdoped regime our results reduce to those of fluctuation theories ($T^* \approx T_c$). Semi-quantitative agreement with Nernst, ac conductivity and diamagnetic measurements is quite reasonable.

PACS numbers: 74.40.+k, 74.25.Fy, 74.72.-h

Keywords: high temperature superconductivity; superconducting fluctuation

The extent to which the normal state of the high T_c superconductors is anomalous has long been debated. The most conclusive evidence for a break-down of Fermi liquid theory has appeared relatively recently via a (pseudo)gap in the fermionic spectrum, with onset temperature T^* . These effects are most apparent with extreme underdoping where $T^*/T_c \gg 1$, whereas in the overdoped regime $T^*/T_c \approx 1$. Recent Nernst[1, 2] and ac conductivity[3] experiments have led to some of the most exotic indications for this pseudogap which, it is claimed, appear in the form of “normal state vortices”. More generally (but not universally[4]) one associates the complex of pseudogap phenomena with some form of precursor superconductivity arising from phase[5] or, alternatively, pair fluctuations[6, 7].

Pair fluctuations are (uncorrelated) non condensed bosons whose dynamics are conventionally modeled[8, 9] using time dependent Ginsburg-Landau (TDGL) theory. When treated self consistently, as in Hartree theory, a fermionic pseudogap necessarily accompanies[10] the appearance of these bosons. TDGL theory, based on strict BCS physics, has met with some success in addressing transport data primarily in overdoped, and possibly, optimal cuprates[8] at both Gaussian[11] and Hartree[9] levels. Here we emphasize that *the very short coherence length of the cuprates suggests that pairing in these materials must take on a non-BCS character* consistent with a superconducting state which is mid-way between BCS and Bose Einstein condensation (BEC)[12, 13]. In this picture T^* is naturally associated with non condensed bosons which owe their origin to a strong pairing attraction g rather than to simple superconducting fluctuations.

In this letter we examine a variety of puzzling experiments which have, in the past, been interpreted as evidence for vortex excitations above T_c . Our purpose is to show that these data are compatible with a preformed pair model, which has as a natural antecedent, TDGL-like physics in the temperature regime around T_c , but which applies to more general $T \leq T^*$. We summarize the key experiments below in terms of the electrical cur-

rent $\mathbf{J}^0 = \sigma \mathbf{E} + \alpha(-\nabla T)$. In contrast to the behavior in a Fermi liquid, a sizeable Nernst signal ν (reflecting a combination of components of the α and σ tensors[2]) appears at an onset temperature appreciably above T_c , called T_ν^* ; this temperature is loosely associated with T^* . In the insulating phase, the thermoelectric response function α_{xy} , as well as ν vanish at $T = 0$. Precursor effects are similarly observed[3] in the imaginary component, σ_2 , of σ at 100 GHz, which set in below T_σ^* , but appreciably above T_c . Thus far, these onset temperatures are significantly below their counterparts for α_{xy} . Moreover, for the range of frequencies measured, these complex conductivity data can be fit[3] to a rescaled Kosterlitz-Thouless form which allows extraction of a phase correlation time $\tau(T)$. In view of the above σ and α experiments, it might seem rather mysterious that the diamagnetic magnetization[2], has a relatively non-existent normal state precursor.

We have in the past considered a pre-formed pair model belonging to a BCS-BEC crossover scheme[7] which can be related[14] to a diagrammatic formulation of the TDGL approach via a common underlying T-matrix formalism. At the Hartree level, the full fermionic Green’s function G appears, so that the pair susceptibility, χ , in this T-matrix depends on[10] GG_o . This is in contrast to Gaussian fluctuations which introduce only bare Green’s functions G_oG_o into χ . Additionally, g is taken to be arbitrary and, consequently, so is T^*/T_c . At a microscopic level, the bosonic contributions are associated with the Aslamazov-Larkin diagram and the fermionic terms with the usual density of states and Maki-Thompson contributions[8], here modified to reflect $\chi \approx GG_o$.

Here we focus on three experiments and temperature regimes where the bosonic contributions are dominant. For the present purposes, it is sufficient to proceed more phenomenologically, while basing our physical picture on these previous microscopic calculations. We consider a system of bosons on a d -dimensional lattice interacting with a bath of (pseudogapped) fermion pairs, which bath we refer to as “reservoir pairs”. We presume, for simplicity, that the reservoir pairs are localized, and that boson-

boson effects are treated at the Hartree level. Here (φ, \mathbf{A}) is the electromagnetic potential, and $\hbar = \epsilon_0 = k_B = 1$:

$$H = \sum_{\mathbf{ux}} \varepsilon_{\mathbf{ux}} \psi_{\mathbf{x}}^\dagger(t) \exp(-iqC_{\mathbf{ux}}(t)) \psi_{\mathbf{x}+\mathbf{u}}(t) + \sum_{\mathbf{x}} q\varphi \psi^\dagger \psi + \sum_{i\mathbf{x}} \left\{ (a_i + q\varphi) w_i^\dagger w_i + \eta_i \psi^\dagger w_i + \eta_i^* w_i^\dagger \psi \right\} + \sum_{i\mathbf{x}} \left\{ (b_i - q\varphi) v_i^\dagger v_i + \zeta_i \psi^\dagger v_i + \zeta_i^* v_i \psi \right\}, \quad (1)$$

where $\varepsilon_{\mathbf{ux}}$ is the hopping matrix element, q is the boson charge, ψ is the annihilation operator for bosons, and w_i and v_i represent annihilation operators for the reservoir pairs, respectively associated with a_i and b_i , which represent sets of positive frequencies. The coupling coefficients η_i and ζ_i are infinitesimal, for each i ; nevertheless, the total contribution from the entire set is arbitrarily large. $C_{\mathbf{ux}}(t) \equiv \int_0^1 ds u_a A_a(\mathbf{x} + s\mathbf{u}, t)$ is a phase factor associated with the electromagnetic vector potential, evaluated on the straight line path connecting two lattice sites. Surface effects appear via the \mathbf{x} dependence of $\varepsilon_{0\mathbf{x}}$. Moreover, $\varepsilon_{0\mathbf{x}}$ contains the Hartree interaction between bosons, which leads to a shift in their chemical potential, μ_{pair} .

The noise spectrum associated with the interaction between the bosons and the reservoir is given by

$$\widetilde{\Sigma}_2(\omega) \equiv 2\pi \sum_i |\eta_i|^2 \delta(\omega - a_i) - 2\pi \sum_i |\zeta_i|^2 \delta(\omega + b_i). \quad (2)$$

We assume that $\widetilde{\Sigma}_2(\omega)$ is smooth and approaches zero as $\omega \rightarrow \pm\infty$. In the zero-field case, the density of the bosons is $\frac{1}{V} \langle \psi^\dagger \psi \rangle = \int \frac{d^d k}{(2\pi)^d} \frac{d\omega}{2\pi} \widetilde{A}(\mathbf{k}\omega) b(\omega)$, where $b(\omega) \equiv 1/(\exp(\omega/T) - 1)$ is the Bose function and V is the volume associated with each lattice site; momentum integrals are confined to the first Brillouin zone throughout and $\widetilde{A}(\mathbf{k}\omega) = \text{Re} 2i\widetilde{\mathcal{T}}(\mathbf{k}\omega)$ is the boson spectral function, where the boson propagator or ‘‘T-matrix’’ is given by

$$\widetilde{\mathcal{T}}(\mathbf{k}\omega) \equiv \left(\omega - \widetilde{\Sigma}_1(\omega) - \varepsilon(\mathbf{k}) + \frac{i}{2} \widetilde{\Sigma}_2(\omega) \right)^{-1}. \quad (3)$$

Here $\varepsilon(\mathbf{k}) \equiv \sum_{\mathbf{u}} \varepsilon_{\mathbf{u}} \exp(ik_a u_a)$ is the boson dispersion, and $\widetilde{\Sigma}_1(\omega) \equiv P \int \frac{d\omega'}{2\pi} \frac{1}{\omega - \omega'} \widetilde{\Sigma}_2(\omega')$. Essential new and microscopically-based physics enters via the temperature dependence of the boson chemical potential $\mu_{\text{pair}}(T) = \max_{\mathbf{k}} (\widetilde{\mathcal{T}}(\mathbf{k}, 0)^{-1})$ which will necessarily depend on the input parameter T^* .

From charge and energy conservation, we can derive the expression for the electric current \mathbf{J}^0 and heat current \mathbf{J}^1 :

$$J_a^n(\mathbf{x}t) = \frac{q^{1-n}}{2V} \left\{ \left(i \frac{\partial}{\partial t} - q\varphi(\mathbf{x}t) \right)^n \psi(\mathbf{x}t) \right\}^\dagger \cdot \sum_{\mathbf{u}} iu^a \varepsilon_{\mathbf{ux}} \exp(-iqC_{\mathbf{ux}}(t)) \psi_{\mathbf{x}+\mathbf{u}}(t) + \text{h.c.} \quad (4)$$

When a small magnetic field $B_{ab} \equiv \frac{\partial}{\partial x_a} A_b - \frac{\partial}{\partial x_b} A_a$ is applied to the system, surface electric and heat currents appear in a thin shell around its boundary. This leads to

$$M_{ab}^n = \frac{q^{2-n}}{6} B_{cd} \int \frac{d^d k}{(2\pi)^d} \frac{d\omega}{2\pi} \Delta_{abcd} \text{Re} i \widetilde{\mathcal{T}}(\mathbf{k}\omega)^2 \omega^n b(\omega), \quad (5)$$

where M_{ab}^0 is the usual magnetization, M_{ab}^1 is the thermal analogue[15] of M_{ab}^0 , $\Delta_{abcd}(\mathbf{k}) \equiv \frac{1}{2}(v_{ac}(\mathbf{k})v_{bd}(\mathbf{k}) - v_{ad}(\mathbf{k})v_{bc}(\mathbf{k}))$, and $v_{ab}(\mathbf{k}) \equiv \frac{\partial^2}{\partial k_a \partial k_b} \varepsilon(\mathbf{k})$ is the inverse mass tensor of the bosons, whose group velocity is given by $v_a(\mathbf{k}) \equiv \frac{\partial}{\partial k_a} \varepsilon(\mathbf{k})$.

For small, but constant magnetic field B_{ab} , electric field $E_a^0 \equiv E_a$, and negative thermal gradient $E_a^1 \equiv -\frac{\partial}{\partial x_a} T$, we can solve the (boson) operator equations of motion to yield the appropriate currents. In the bulk volume the corresponding expectation value is \mathbf{J}^n . However, the physically measured or ‘‘transport’’ currents contain contributions from the surface, and are given by:

$$J_{(\text{tr})a}^n = \langle J_a^n \rangle + \frac{\partial M_{ab}^n}{\partial T} E_b^1 + \delta_{n,1} M_{ab}^0 E_b^0. \quad (6)$$

The DC transport coefficients, defined by $J_{(\text{tr})a}^n = \sum_{n'=0}^1 \sum_b L_{ab}^{nn'} E_b^{n'}$, (which are readily related to α, σ) turn out to be

$$L_{ab}^{nn'} = \frac{q^{2-n-n'}}{2T^{n'}} \int \frac{d^d k}{(2\pi)^d} \frac{d\omega}{2\pi} v_a v_b \widetilde{A}^2 \omega^{n+n'} b^{(1)} + \frac{q^{3-n-n'}}{6T^{n'}} B_{cd} \int \frac{d^d k}{(2\pi)^d} \frac{d\omega}{2\pi} v_a v_c v_{bd} \widetilde{A}^3 \omega^{n+n'} b^{(1)}, \quad (7)$$

where $b^{(1)}(\omega) \equiv -\frac{\partial b(\omega)}{\partial \omega}$, $L_{ab}^{00} = \sigma_{ab}$ is the isothermal electric conductivity, L_{ab}^{11} is the isoelectropotential thermal conductivity, and $L_{ab}^{01} = \alpha_{ab}$ and L_{ab}^{10} are off-diagonal coefficients. Eq. (7) satisfies the Onsager relation $T^{n'} L_{ab}^{nn'}(\vec{B}) = T^n L_{ba}^{n'n}(-\vec{B})$ (no summation), as a consequence of our inclusion of the surface terms[11]. Surface effects enter into L_{ab}^{01} , L_{ab}^{10} and L_{ab}^{11} , but not L_{ab}^{00} .

Finally, we deduce the boson contribution to the complex ac conductivity

$$\begin{aligned} \tilde{\sigma}_{ab}(\omega) &= \frac{iq^2}{\omega} \int \frac{d^d k'}{(2\pi)^d} \frac{d\omega'}{2\pi} v_a(\mathbf{k}') v_b(\mathbf{k}') \widetilde{A}(\mathbf{k}'\omega') b(\omega') \\ &\cdot (\widetilde{\mathcal{T}}(\mathbf{k}', \omega' + \omega) + \widetilde{\mathcal{T}}^*(\mathbf{k}', \omega' - \omega) - \widetilde{\mathcal{T}}(\mathbf{k}'\omega') - \widetilde{\mathcal{T}}^*(\mathbf{k}'\omega')) \\ &+ \frac{iq^3}{2\omega} B_{cd} \int \frac{d^d k'}{(2\pi)^d} \frac{d\omega'}{2\pi} v_a(\mathbf{k}') v_c(\mathbf{k}') v_{bd}(\mathbf{k}') \widetilde{A}(\mathbf{k}'\omega') b(\omega') \\ &\cdot (i\widetilde{\mathcal{T}}(\mathbf{k}', \omega' + \omega) - i\widetilde{\mathcal{T}}^*(\mathbf{k}', \omega' - \omega)) \\ &\cdot (\widetilde{\mathcal{T}}(\mathbf{k}', \omega' + \omega) + \widetilde{\mathcal{T}}^*(\mathbf{k}', \omega' - \omega) - \widetilde{\mathcal{T}}(\mathbf{k}'\omega') - \widetilde{\mathcal{T}}^*(\mathbf{k}'\omega')). \end{aligned} \quad (8)$$

It can be verified that $\tilde{\sigma}_{ab}(\omega \rightarrow 0) = L_{ab}^{00}$ and that Eq. (8) satisfies the f-sum rule.

Our numerical evaluation[16] of these transport coefficients makes use of the fact that the integrals over momentum in Eqs. (7) and (8) can be reduced to integrals over a single energy variable by introducing generalized density of states functions associated with the bosons' dispersion. We presume that T^*/T_c (which is roughly fitted to the phase diagram) is the principle input parameter rather than hole concentration x , or coupling constant g . Essential to this theory is the temperature dependence of the boson chemical potential $\mu_{\text{pair}}(T)$ which, is chosen so that the boson number is zero above T^* . This should be contrasted with the TDGL result $\mu_{\text{pair}} \propto (T - T_c)$ which holds only near Bose condensation[16], and generally tends to overestimate bosonic effects away from T_c .

In Fig. 1 is plotted the transverse thermoelectric coefficient α_{xy} vs T for three underdoped samples with indicated T^*/T_c . The arrows show the corresponding values of T_c which progressively decrease as T^*/T_c increases. The inset plots (unpublished) experimental data on $\text{La}_{2-x}\text{Sr}_x\text{CuO}_4$ from Ref. 17 which curves are for $x = 0.12, 0.07$, and 0.03 and which are in rough correspondence to the values of T^*/T_c in the three theory plots. In both theory and experiment the dotted lines are for a non-superconductor $T_c = 0$. If we estimate the onset temperatures for α_{xy} , called T_α^* , using the experimental data to calibrate the fermionic background, we find T^*/T_α^* is given by 1.3, 1.7, and 2.6 for the solid, dashed and dotted curves, respectively. These onsets are of the order of $T^*/2$, as in experiment. In the vicinity of T_c , the calculated behavior of α_{xy} corresponds to that of TDGL theory, albeit with modified coefficients. Thus α_{xy} diverges at T_c although ν is finite there[11]. Similarly, with overdoping the behavior becomes characteristic of a more conventional fluctuation picture in which $T^* \approx T_c$. The essential distinction between TDGL and the present case is that the onset temperature for bosonic contributions can be substantially higher than the critical fluctuation regime. This figure illustrates the fact that α_{xy} (as well as ν) vanish at $T = 0$ in non-superconducting samples. This derives from the behavior of the Bose factor which has vanishing first derivative at $T = 0$. Semi-quantitative agreement between theory and experiment appears quite satisfactory.

An interesting inference from the data[2] is that, while, there is a considerable precursor effect for α_{xy} , the (orbital) magnetization drops to its superconducting value only in the immediate vicinity of Bose condensation. This quantity [given as M_{ab}^0 in Eq. (5)] is plotted in the inset to Fig. 2, for the same parameter set as in Fig. 1. The fermionic background (measured experimentally) is negligible, so that the bosonic contribution necessarily dominates. The sharpness of the Meissner onset (which clearly reflects T_c and not T^*) can be attributed to the small ratio of the boson velocity to the speed of light (and the small size of the hyperfine constant). Similar results hold in TDGL-based calculations.

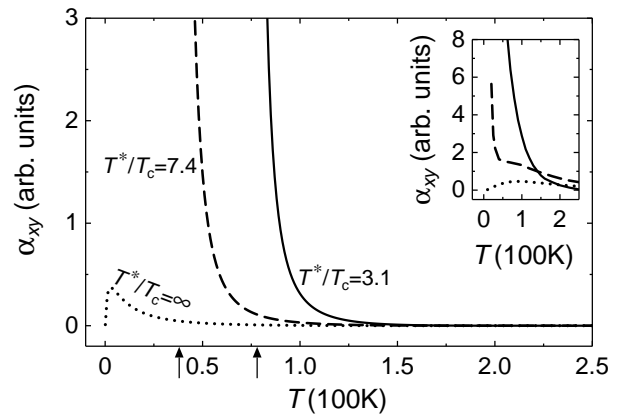


FIG. 1: Theoretical curves for the normal state α_{xy} with variable T^*/T_c ; experimental counterparts[17] in inset for $\text{La}_{2-x}\text{Sr}_x\text{CuO}_4$ at $x = 0.03, 0.07$, and 0.12 .

In the main body of Fig. 2 are plotted the real and imaginary components of the ac conductivity as a function of T for $\omega \approx 100$ GHz for two different values of T^*/T_c , as in the previous figure. Both $\sigma_1 = \text{Re}\sigma$ and $\sigma_2 = \text{Im}\sigma$ are finite at T_c with σ_2 only slightly larger than σ_1 . The associated frequency dependence reflects the well known[8] $1/\sqrt{\omega}$ behavior of TDGL. It follows from TDGL that $d\sigma_1/dT$ is finite while $d\sigma_2/dT$ diverges at T_c . This latter prediction is the most notable difference between theory and experiment[3], although small sample inhomogeneities may smooth out a derivative divergence in the data. The theoretically deduced onset temperature T_σ^* , for precursor effects in σ_2 can be estimated by noting that the fermionic background is relatively negligible so that σ_2 becomes appreciable when it reaches a few percent of its value at T_c . This corresponds to onset temperatures which are factors of 2 or so below those estimated from α_{xy} .

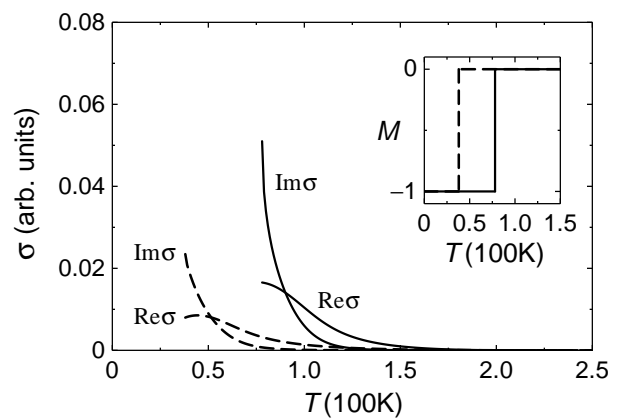


FIG. 2: Real and imaginary components of normal state σ at 100 GHz vs T . Solid and dashed curves have same T^*/T_c as for counterparts in Fig. 1. Associated magnetizations are plotted in inset.

Finally, in Fig. 3 we replot the calculated ac conductivity following the Kosterlitz-Thouless (KT) based analysis of Ref.3. Fits to KT physics are the basis of an interpretation of these conductivity data in terms of vortices above T_c . In the main figure are plotted $\phi \equiv \tan^{-1}(\sigma_2/\sigma_1)$ and $|S|$ as a function of ω/Ω obtained from fitting the KT scaling formula $\sigma(\omega) \propto T_\theta^0(T)S(\omega/\Omega)\Omega^{-1}$. As in the data, here, T_θ^0 and Ω are deduced parameters. The inset plots $\tau = 1/\Omega$ as a function of temperature. We find that T_θ^0 is roughly constant in T , in contrast to the data which finds this quantity to be decreasing as T increases. Nevertheless, the agreement with experiment for all three quantities plotted in Fig. 3 is quite good. In this way one might argue that key features of the data in Ref. 3 and attributed to KT physics, may equally well be explained by pre-formed pairs.

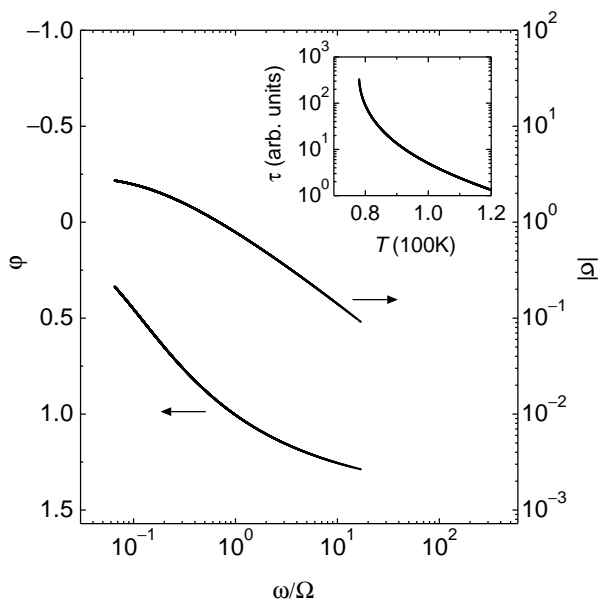


FIG. 3: Fits to Kosterlitz-Thouless (KT) scaling of the conductivity. See text for details.

In this letter we have built on previously successful[8, 9, 11] applications of TDGL physics to the overdoped cuprates. This work has set the stage for our focus on non-condensed bosons in the form of pre-formed pairs (associated with strong pairing attraction, rather than superconducting fluctuations) with onset at arbitrary T^*/T_c . Equations (7) and (8) are the important results of this letter; they provide exact and general expressions for transport coefficients associated with these non-

condensed bosons, and which, near T_c reduce to those of TDGL theory, albeit with a non-BCS parameter set. We have focused on three experiments in underdoped cuprates, two of which have been previously argued to provide support for vortex excitations above T_c . We believe the reasonable agreement between theory and experiment provides support for a preformed-pair alternative to the vortex scenario.

Work supported by NSF-MRSEC Grant No.DMR-0213745. We thank Y. Wang and N. P. Ong for unpublished data, and G. Mazenko for useful conversations.

-
- [1] Z. Xu, N. Ong, Y. Wang, T. Kakeshita, and S. Uchida, *Nature* **406**, 486 (2000).
 - [2] Y. Wang, Z. A. Xu, T. Kakeshita, S. Uchida, S. Ono, Y. Ando, and N. P. Ong, *Phys. Rev. B* **64**, 224519 (2001).
 - [3] J. Corson, R. Malozzi, J. Orenstein, J. N. Eckstein, and I. Bozovic, *Nature* **398**, 221 (1999).
 - [4] S. Chakravarty, R. B. Laughlin, D. K. Morr, and C. Nayak, *Phys. Rev. B* **63**, 094503 (2001).
 - [5] V. J. Emery and S. A. Kivelson, *Nature* **374**, 434 (1995).
 - [6] M. Randeria, in *Bose Einstein Condensation*, edited by A. Griffin, D. Snoke, and S. Stringari (Cambridge Univ. Press, Cambridge, 1995), pp. 355–92.
 - [7] Q. J. Chen, I. Kosztin, B. Janko, and K. Levin, *Phys. Rev. Lett.* **81**, 4708 (1998).
 - [8] A. Larkin and A. Varlamov (2001), cond-Mat/0109177.
 - [9] S. Ullah and A. T. Dorsey, *Phys. Rev. B* **44**, 262 (1991).
 - [10] B. R. Patton, *Phys. Rev. Lett.* **27**, 1273 (1971).
 - [11] I. Ussishkin, S. Sondhi, and D. Huse, *Phys. Rev. Lett.* **89**, 287001 (2002).
 - [12] A. J. Leggett, in *Modern Trends in the Theory of Condensed Matter* (Springer-Verlag, Berlin, 1980), pp. 13–27.
 - [13] P. Nozières and S. Schmitt-Rink, *J. Low Temp. Phys.* **59**, 195 (1985).
 - [14] Jelena Stajic and K. Levin, unpublished.
 - [15] In the present case there is no particle-hole symmetry and we consider T away from T_c so that the thermal surface magnetization is non-zero.
 - [16] Our parameter set is: $T_c = \max(0, T')$, where $T' = 1.6T^* - 0.5T^{*2} - 0.18$; $\gamma = \gamma_1 + \gamma_2 i$, where $\gamma_1 = 0.01 + 0.1(1 - T'/T^*)$, and $\gamma_2 = 5 + 10T'/T^*$; $\tilde{\Sigma}_2(\omega) = \frac{200p_2\omega}{(\omega - p_1)^2 + p_2^2}$, where $p_1 = \text{Re}p$, $p_2 = \text{Im}p$, and $p = \frac{100}{\gamma^* - 1}$; $\tilde{\Sigma}_1(0) + \varepsilon(\mathbf{k}) = a(T) + \mathcal{E}_1(1 - \cos(k_1 l_1)) + \mathcal{E}_1(1 - \cos(k_2 l_2)) + \mathcal{E}_3(1 - \cos(k_3 l_3))$, $\mathcal{E}_3/\mathcal{E}_1 = 10^{-4}$, and $a(T) = -\mu_{\text{pair}} = \frac{(T^* - T')^2(T - T')^2}{(T^* - T)^2} + \frac{T'^2(T - T')}{T^{*2}}$.
 - [17] Yayu Wang and N. P. Ong, private communication.